Effect of Pedestrian Buck Contact Area and Force-Deflection Property on Pedestrian Pelvis and Lower Limb Injuries

Miwako Ikeda[1], Shunji Suzuki[1], Yukou Takahashi[1], Shinsuke Oda[2],
Rikard Fredriksson[3], Bengt Pipkorn[3]

Abstract In order to develop requirements for designing a pedestrian buck, this study conducted two parametric studies that investigated the effect of the vehicle stiffness characteristics and the area of contact between the pedestrian pelvis and lower limb and a vehicle on pedestrian pelvis and lower limb injury measures. The parametric study for different vehicle stiffness characteristics was conducted using a human finite element (FE) model and simplified vehicle models with different front shapes for which stiffness parameters were varied. With regard to the contact area, a prescribed force model representing the contact force time histories from a vehicle was developed and applied to the human FE model, without using a vehicle model, to allow change in the contact area while maintaining the total force magnitude. It was found that maintaining the peak force magnitude is much more important than the maximum deflection of the stiffness characteristics and that accurate representation of the impacted body region is much more significant than the contact area, in reproducing the maximum injury measures.

Keywords Buck, Contact area, Finite Element Method, Injury, Pedestrians

I. INTRODUCTION

Pedestrian protection has been one of the major issues in traffic safety in the world [1]. For the purpose of mitigating pedestrian injuries, many studies have been conducted in an attempt to clarify injury mechanisms in car-to-pedestrian accidents. As one of such efforts, a full-scale pedestrian dummy has been developed that represents a mid-sized male [2]. In addition, information reports have been developed and published under the auspices of the Society of Automotive Engineers Human Biomechanics And Simulations Standards Steering Committee that specify performance specifications for full-body pedestrian dummies, including the whole body kinematics and the biofidelity at the component level [3][4]. In one of the information reports (J2868), an example is presented with regard to the trajectory corridors of different body segments obtained from the full-scale car-pedestrian impact tests using Post Mortem Human Subjects (PMHSs) and a vehicle buck. Since the vehicle buck used in this experiment represents a specific passenger vehicle, questions have been raised on the specific vehicle used, in terms of both the future availability of the vehicle and the representativeness of the vehicle in real world car-pedestrian collisions.

In order to address this issue, some of the past studies attempted to develop pedestrian bucks that represent the vehicle front shape and stiffness characteristics with simple structures. Untaroiu et al. [5] developed two FE models of pedestrian bucks that represent a mid-sized sedan and a large sedan, and conducted impact simulations using a pedestrian dummy FE model against a full vehicle FE model along with the pedestrian buck FE model representing the corresponding vehicle. They confirmed a good correlation of the upper body kinematics between the full vehicle and buck models. Similarly, Suzuki et al. [6] conducted car-pedestrian impact simulations using a human FE model against the full vehicle and buck FE models used by Untaroiu et al. for representing a mid-sized sedan, and compared the upper body kinematics and pelvis and lower limb injury measures. It was found that the upper body kinematics and the wave profiles of the injury measure time histories matched well with the vehicle and buck models. However, it was also concluded that the geometric and stiffness characteristics along with the rate sensitivity, effective mass and crash stroke of

Miwako Ikeda is Engineer (e-mail; miwako_ikeda@n.t.rd.honda.co.jp), Shunji Suzuki is Assistant Chief Engineer (e-mail; shunji_suzuki@n.t.rd.honda.co.jp), and Yukou Takahashi is Chief Engineer (e-mail; yukou_takahashi@n.t.rd.honda.co.jp) at Honda R&D Co., Ltd. Automobile R&D Center in Japan (tel; +81-28-677-3311). Shinsuke Oda is Technical manager at Autoliv Japan Ltd. (e-mail; shinsuke.oda@autoliv.com, tel; +81-45-475-3989). Rikard Fredriksson is Research Engineer (email; rikard.fredriksson@autoliv.com), and Bengt Pipkorn is Technical Specialist (email; bengt.pipkorn@autoliv.com) at Autoliv Research (tel; +46-322-626300).

some of the components of the pedestrian buck need to be modified in order to more accurately reproduce time histories of the pelvis and lower limb injury measures. Takahashi et al. [7][8] developed simplified vehicle models representing three different types of vehicles with simple structures for investigating the effect of simplification of stiffness characteristics of front-end structures on pedestrian injury measures in car-pedestrian collisions. They found that the maximum injury measures highly depend on the peak force magnitude, and that maximum injury measures for the pelvis and lower limb could be reproduced with the accuracy of ±10% provided that the peak force magnitude and the deflection and the absorbed energy up to the peak force were conserved, regardless of the stiffness curves up to the peak force. Although the study provided a guideline for the stiffness characteristics of a pedestrian buck by showing the significance of some of the stiffness parameters, the relationship between the accuracy of the representation of these stiffness parameters and the accuracy of the injury measure prediction still requires further clarifications, since such information is deemed necessary when developing an actual pedestrian buck with a certain target of the accuracy of the injury measure prediction. In addition, the effect of the contact area still needs to be investigated, considering the difficulties in precisely reproducing the contact area time histories using simplified buck components.

The goal of this study was to quantitatively investigate the effect of the change in the peak force magnitude and the deflection at the peak force, and the effect of the change in the contact area between the pedestrian and the vehicle, on pedestrian pelvis and lower limb injury measures.

II. METHODS

Effect of Change in Peak Force Magnitude and Deflection at Peak Force

Vehicle Models: Simplified vehicle models used in this study were taken from those developed in our previous study by Takahashi et al. [7] (Fig. 1). Three types of vehicles with different front shapes were selected in order to represent different loading patterns to the pelvis of a pedestrian. Vehicle A representing a sedan-type vehicle simulated the pelvis loading through the acetabulum due to direct loading to the leg and thigh. Vehicle B representing an SUV reproduced the pelvis loading through the acetabulum due to direct loading to the greater trochanter. Vehicle C representing a minivan represented the direct loading to the iliac wing. Each model consisted of four components: the hood, the grille, the bumper, and the bumper lower (the lower part of the bumper). These components were modeled as rigid bodies and were connected via springs to a node to which the mass was added in such a way that the total mass of the vehicle model is identical to that of the actual vehicle. In terms of the degree of freedom of the motion of each component, the motion in the x-direction (vehicle longitudinal direction) was allowed for all the vehicles and their components. Since the result of the previous study using an FE full vehicle model showed that the peak contact force in the z-direction from the hood was significant for Vehicle A, the motion in the z-direction (vertical direction) of the hood of Vehicle A was also set free. A multi-linear representation of the stiffness curves that was found to be able to reproduce most of peak pelvis and lower limb injury measures within 15% was used to determine the baseline stiffness curves. Fig.2 shows an example of the stiffness curves (Grille of Vehicle A in the x-direction).

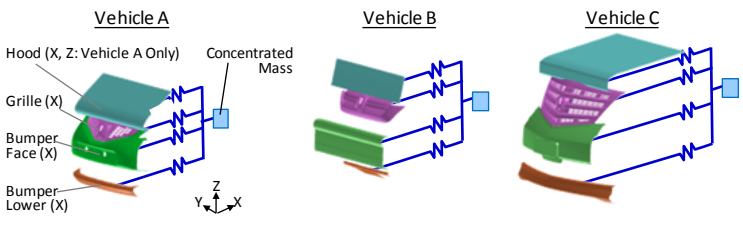

Fig. 1. Simplified Vehicle Models

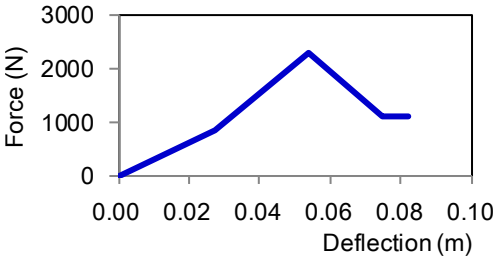

Fig. 2. Multi-linear Representation of Stiffness Curves

Human FE Model: A human FE model representing a mid-sized male pedestrian used in this study was developed by Takahashi et al. [9] and Ikeda et al. [10] (Fig.3). The pelvis and the lower limb were modeled using shell and solid elements to accurately represent the geometry of these body regions. The material property and failure characteristics were determined from the literature, and were validated against published quasi-static

and dynamic tests using human subjects. The model validation included the lateral compression of the pelvis in acetabulum and iliac loadings, 3-point bending of the thigh, femur, leg, tibia and fibula at multiple loading locations, tension of the individual knee ligament, and 4-point bending of an isolated knee joint. The upper part of the body was modeled using articulated rigid bodies with all of the seven cervical and five lumbar vertebrae modeled to represent the flexibility of these regions. The full-body pedestrian model was also validated against published full-scale car-pedestrian impact experiments in terms of the trajectories of the head, T1, T8 and pelvis along with the pelvis and lower limb injury prediction in collisions with a small sedan and a large SUV.

Impact Simulation: Impact simulations were conducted using PAM-CRASH by impacting the human FE model in a standing position with the simplified vehicle models. The pedestrian model was hit laterally from the left by the three simplified vehicle models at 40 km/h. The lower limbs were rotated about the latero-medial axis by 10° with the right limb forward to represent a gait stance. As an example, Fig.4 shows a schematic of the impact simulation for Vehicle A.

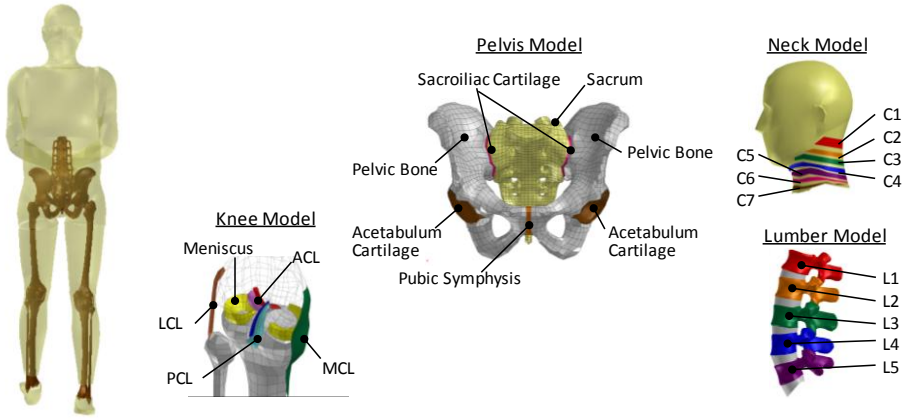

Fig. 3. Human FE Model

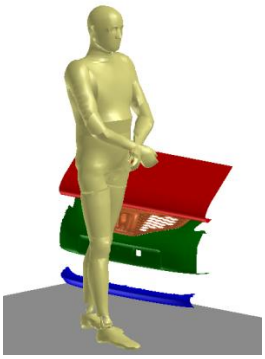

Fig. 4. Schematic of Impact Simulation

Injury Measures: Similar to the previous studies [6][7][8], four injury parameters were selected for predicting pelvis and lower limb injury levels of a pedestrian: the deformation between the left and right acetabula for pubic rami fracture, femur and tibia bending moments for fracture of these bones, and MCL (Medial Collateral Ligament) elongation for MCL failure. The locations at which these measures were recorded are shown in Fig. 5.

Parametric Study: In order to quantitatively investigate the effect of the change in the peak force magnitude and the deflection at the peak force of the stiffness characteristics on the pelvis and lower limb injury measures, a parametric study using the simplified vehicle models was conducted. As shown in Fig.6, the stiffness curve of each component was scaled in the vertical (force) and horizontal (deflection) directions individually by ±10% and ±20%. 40 cases (8 stiffness curves x 5 components/directions) and 32 cases (8 stiffness characteristics x 4 components) of the impact simulation were performed for Vehicle A and Vehicles B and C, respectively. The pelvis and lower limb injury measures from the results of these impact simulations were compared to those from the results of the baseline model.

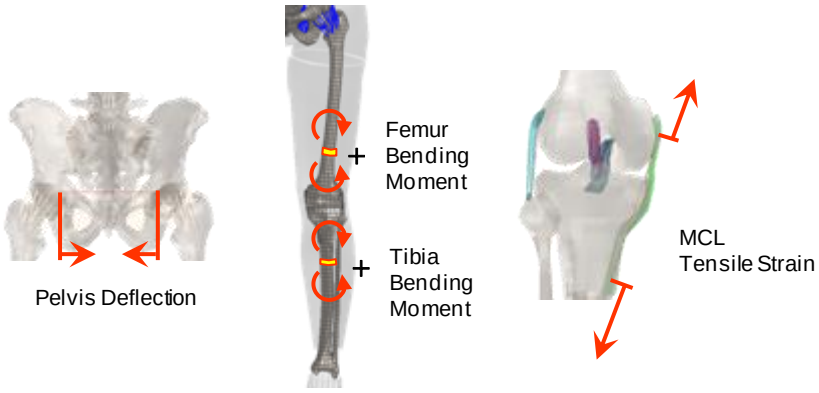

Fig. 5. Location of Injury Measurements

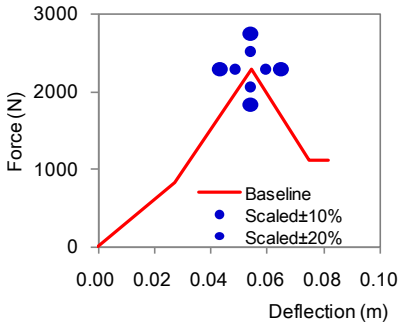

Fig. 6. Scaling of Stiffness Curve used for Parametric Study

Effect of Change in Contact Area

Development of Baseline Prescribed Force-Time Model: Since the contact area between a pedestrian and a vehicle varies during a collision, it is impossible to isolate the effect of the contact area from the impact simulations using vehicle models. In order to purely isolate the effect of the contact area while maintaining the magnitude of the applied force, this study developed a methodology to model the forces applied to a pedestrian from a vehicle without using a vehicle model. The baseline Prescribed Force-Time (PFT) model was developed, for which prescribed force time histories were directly applied to the nodes of a surface of the human FE model. Since the load generated by the contact with a vehicle was represented by a prescribed force time history, no vehicle model was used for the PFT model. The baseline PFT model was developed for each vehicle using the following procedure:

1. The distribution of the contact pressure and the time histories of the contact area and contact force magnitude were identified for each combination of the pedestrian body region and the component of the vehicle from the impact simulation using a full FE vehicle model.
2. The contact area on the surface of the human FE model was divided into small regions based on the distribution of the contact pressure at the time of the peak force generated by each component.
3. The time histories of the contact force for each combination of the small region and the vehicle component were calculated.
4. The prescribed force time histories determined in step 3 were evenly distributed among the nodes constituting each small region of the human FE model.
5. Peak injury measures from the model obtained in step 4 were compared to those from the impact simulation using the full FE vehicle model to calculate the difference of the peak measures.
6. Steps 2 through 5 were repeated until all the differences in the injury measures fell within ±15% of the results from the full FE vehicle model.

The threshold of the difference was determined as 15% with reference to the development of the simplified vehicle models in the previous study. Since Takahashi et al. [9] found that the peak pelvis injury measure is affected by the effective mass of the contralateral lower limb, the regions on the right (contralateral) limb were also investigated. The segmentations of the small regions are shown in Figs.7 through 9 for Vehicles A, B and C, respectively. The comparisons of the injury measures between the full FE vehicle model and the baseline PFT model are shown in TABLE I and Fig.10.

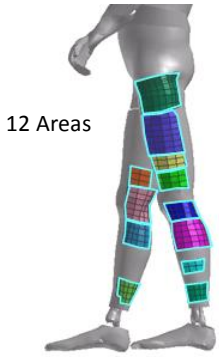

Fig. 7. Segmentation of Small Region in Baseline PFT Model for Vehicle A

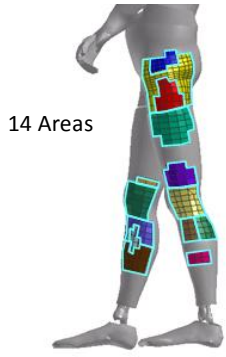

Fig. 8. Segmentation of Small Region in Baseline PFT Model for Vehicle B

Fig. 9. Segmentation of Small Region in Baseline PFT Model for Vehicle C

TABLE I

COMPARISON OF PEAK INJURY MEASURES BETWEEN FULL FE VEHICLE MODEL AND PFT MODEL

	Pelvis Deformation (mm) and Difference			Femur Bending Moment (Nm) and Difference			MCL Tensile Strain (-) and Difference			Tibia Bending Moment (Nm) and Difference		
	FE	Baseline PFT	Difference	FE	Baseline PFT	Difference	FE	Baseline PFT	Difference	FE	Baseline PFT	Difference
Vehicle A	1.59	1.71	7.5%	264	253	-4.2%	0.101	0.092	-8.9%	242	230	-5.0%
Vehicle B	5.48	5.42	-1.1%	272	265	-2.6%	0.106	0.118	11.3%	274	249	-9.1%
Vehicle C	4.8	4.31	-10.2%	194	216	11.3%	0.089	0.101	13.5%	265	246	-7.2%

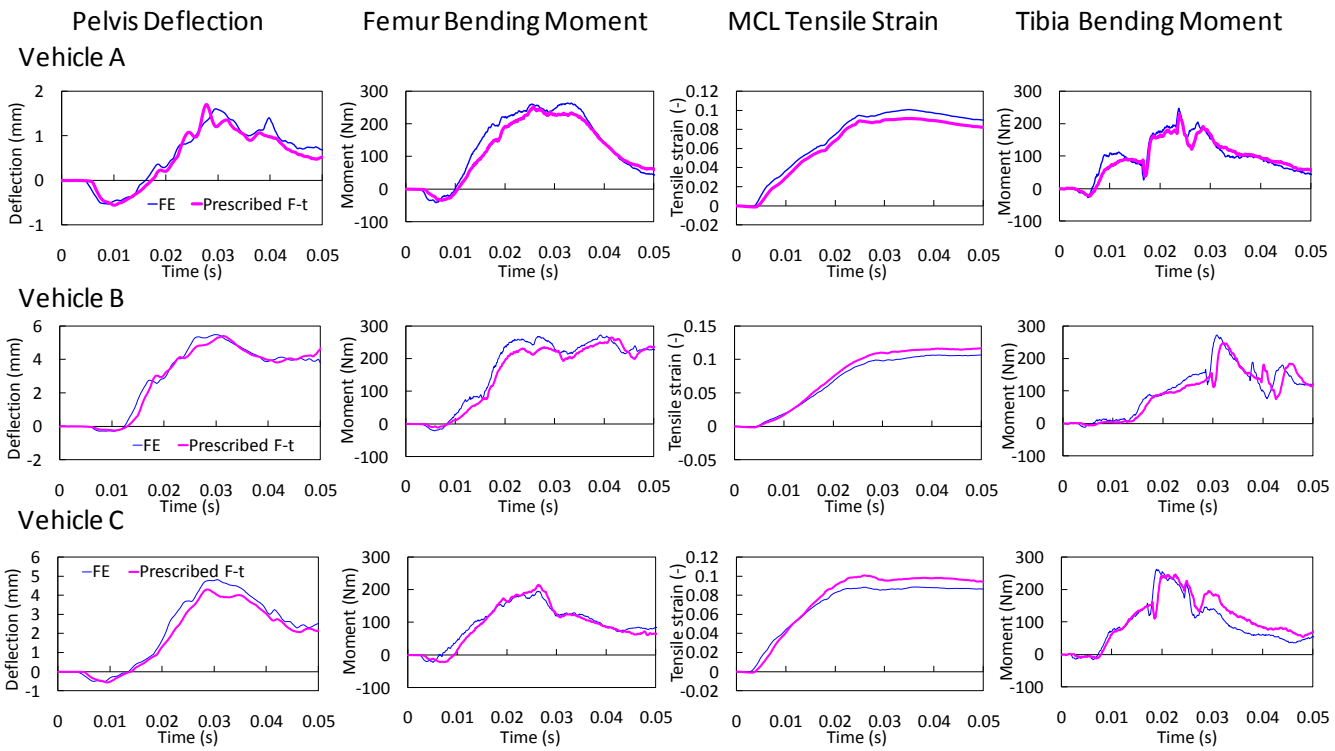

Fig. 10. Comparison of Injury Measure Time Histories between Full FE Vehicle Models and Baseline PFT Models

Parametric Study: In order to quantitatively investigate the effect of the contact area generated by the contact between a pedestrian and each component of a vehicle on the pelvis and lower limb injury measures, a parametric study was conducted using the PFT models.

The levels of the contact area used in this parametric study were determined by the following procedure:

1. The time history of the contact area was determined for each combination of the pedestrian body region and the vehicle component from the impact simulation using a full FE vehicle model.
2. The time window up to the peak contact area was divided into three equal parts.
3. The levels of the contact area were determined from the average in each time part. The levels of the contact area were denoted as Averaged Area-1, 2 and 3, respectively (Fig.11).

The contact area at the level of Averaged Area-3 was redefined by the following procedure;

1. The regions on the surface of the pedestrian body where the contact pressure generated by each component of the vehicle at the time of the peak contact force was distributed were identified from the impact simulation using the full FE vehicle model.
2. The highest and lowest ends of the region identified in step 1 were determined to calculate the vertical distance of the ends of the region.
3. Averaged Area-3 was divided by the vertical distance determined in step 2 to calculate the width of the redefined contact area.
4. The center line on the surface of the pedestrian body along the axis of the lower limb was transferred in the anterior and posterior directions on the surface of the pedestrian body by half of the width defined in step 3 to determine the anterior and posterior borders of the contact area.
5. The area surrounded by the borders determined in steps 2 and 4 was used as the contact area for Case A3.

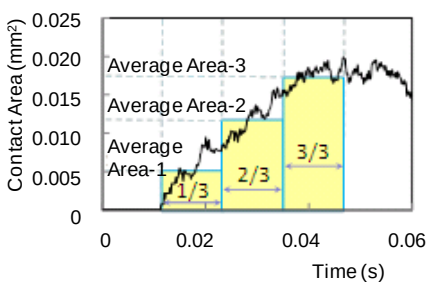

Fig. 11. Example of Time History of Contact Area

This redefinition of the contact area was necessary to change the contact area between Averaged Area-1, 2 and 3 in a consistent manner. Since Averaged Area-1 and 2 are smaller than Averaged Area-3, the locations of contact area at the levels of Averaged Area-1 and 2 were defined by the following procedure;

1. Two vertically different locations of the contact area for Averaged Area-1 and 2 were determined.
2. The same anterior and posterior borders of the contact area as those for Averaged Area-3 were used for Averaged Area-1 or 2 as well.
3. For the upper and lower locations of the contact area for Averaged Area-1 and 2, the lower and upper borders were determined in such a way that the upper and lower borders of the contact area redefined for Averaged Area-3, respectively, were used, and the area coincides with Averaged Area-1 and 2 (Cases A1-U and A2-U for the upper location, Cases A1-L and A2-L for the lower location).

Since Averaged Area-3 for the bumper lower was significantly smaller than those for the other components in all vehicles, the effect of the size of the contact area of the bumper lower was not investigated in this parametric study. In addition, since Averaged Area-3 for the grille and bumper were significantly smaller than those for the hood in all vehicles, only Cases A1-U, A1-L, and A3 were selected for the grille and bumper in the parametric study. The force-time history to be applied to the nodes in each contact area defined above was determined in such a way that the total force applied to the small regions of the baseline PFT model representing the contact with the corresponding vehicle component was evenly distributed among the nodes. The combinations of the component and the level of the contact area are shown in TABLE II. The location of the contact area in Cases H-A1-U, H-A1-L, G-A1-U, G-A1-L, B-A1-U, and B-A1-L is shown in Figs.12 through 14.

TABLE II

COMBINATIONS OF THE COMPONENT AND THE LEVEL OF CONTACT AREA

Case ID	Component	Level of Contact Area	Location in the A3	Case ID	Component	Level of Contact Area	Location in the A3
H-A1-U	Hood	A1	Upper	G-A1-U	Grille	A1	Upper
H-A1-L	Hood	A1	Lower	G-A1-L	Grille	A1	Lower
H-A2-U	Hood	A2	Upper	G-A3	Grille	A3	-
H-A2-L	Hood	A2	Lower	B-A1-U	Bumper	A1	Upper
H-A3	Hood	A3	-	B-A1-L	Bumper	A1	Lower
-	-	-	-	B-A3	Bumper	A3	-

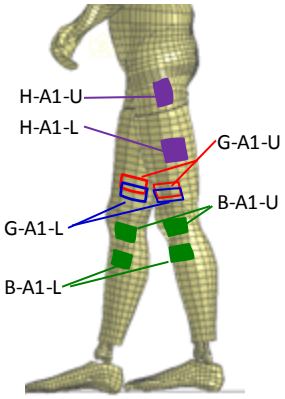

Fig. 12. Locations of the Contact Area for Vehicle A

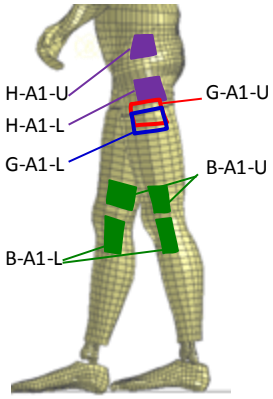

Fig. 13. Locations of the Contact Area for Vehicle B

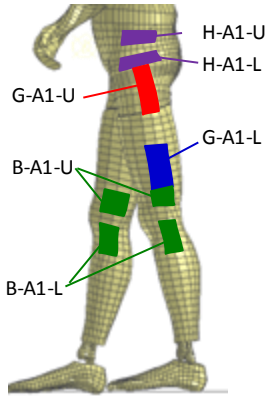

Fig. 14. Location of the Contact Area for Vehicle C

III. RESULTS

Effect of Change in Peak Force Magnitude and Deflection at Peak Force

The comparisons of the injury measures for the pelvis and lower limb are summarized in TABLEs III through VIII.

In the cases using the stiffness curves scaled in the direction of the deflection, all differences between these cases and the baseline model were within the range of ±5%. In the cases using the stiffness curves scaled in the direction of the force at the level of ±10%, all differences between these cases and the baseline model were within the range of ±8%.

TABLE III

COMPARISONS OF INJURY MEASURES BETWEEN BASELINE MODEL AND MODELS WITH DIFFERENT STIFFNESS CURVES SCALED IN DEFLECTION FOR VEHICLE A (BPR LWR STANDS FOR BUMPER LOWER)

Component	Scaled Factor	Pelvis Deformation (mm) and Difference		Femur Bending Moment (Nm) and Difference		MCL Tensile Strain (-) and Difference		Tibia Bending Moment (Nm) and Difference	
Baseline	-	1.85	-	280	-	0.097	-	216	-
Hood	-10%	1.85	-0.2%	283	1.2%	0.097	0.2%	216	-0.2%
Grille	-10%	1.84	-0.7%	272	-2.9%	0.097	-0.1%	221	2.5%
Bumper	-10%	1.86	0.4%	275	-1.9%	0.099	1.5%	217	0.4%
BPR LWR	-10%	1.89	2.2%	274	-2.3%	0.098	0.6%	221	2.2%
Hood (Z)	-10%	1.88	1.6%	282	0.6%	0.097	-0.3%	214	-1.0%
Hood	+10%	1.84	-0.3%	277	-0.9%	0.097	0.0%	215	-0.3%
Grille	+10%	1.88	1.7%	285	1.9%	0.099	1.9%	217	0.5%
Bumper	+10%	1.86	0.6%	280	0.1%	0.098	0.2%	217	0.6%
BPR LWR	+10%	1.83	-0.9%	282	0.7%	0.098	0.9%	214	-0.9%
Hood (Z)	+10%	1.84	-0.4%	279	-0.5%	0.098	0.4%	215	-0.2%
Hood	-20%	1.86	0.5%	286	2.3%	0.097	0.2%	217	0.5%
Grille	-20%	1.84	-0.4%	269	-3.8%	0.097	-0.7%	224	3.6%
Bumper	-20%	1.86	0.5%	282	0.9%	0.097	-0.1%	217	0.5%
BPR LWR	-20%	1.86	0.4%	275	-1.9%	0.098	1.0%	217	0.4%
Hood (Z)	-20%	1.91	3.1%	281	0.5%	0.097	-0.7%	216	-0.1%
Hood	+20%	1.85	0.0%	276	-1.4%	0.097	-0.2%	216	0.0%
Grille	+20%	1.91	3.4%	288	2.7%	0.099	1.9%	217	0.3%
Bumper	+20%	1.86	0.5%	279	-0.4%	0.098	0.4%	217	0.5%
BPR LWR	+20%	1.81	-2.2%	283	1.2%	0.098	1.0%	211	-2.2%

TABLE IV

COMPARISONS OF INJURY MEASURES BETWEEN BASELINE MODEL AND MODELS WITH DIFFERENT STIFFNESS CURVES SCALED IN FORCE FOR VEHICLE A (BPR LWR FOR BUMPER LOWER)

Component	Scaled Factor	Pelvis Deformation (mm) and Difference		Femur Bending Moment (Nm) and Difference		MCL Tensile Strain (-) and Difference		Tibia Bending Moment (Nm) and Difference	
Baseline	-	1.85	-	280	-	0.097	-	216	-
Hood	-10%	1.84	-0.4%	278	-0.7%	0.097	-0.5%	215	-0.4%
Grille	-10%	1.82	-1.6%	265	-5.4%	0.097	-0.1%	219	1.5%
Bumper	-10%	1.73	-6.5%	275	-1.8%	0.097	-0.6%	202	-6.5%
BPR LWR	-10%	1.82	-1.4%	285	2.0%	0.098	0.6%	213	-1.4%
Hood (Z)	-10%	1.83	-1.2%	279	-0.4%	0.098	0.6%	217	0.5%
Hood	+10%	1.87	1.0%	283	1.1%	0.098	0.7%	218	1.0%
Grille	+10%	1.90	2.5%	289	3.2%	0.099	1.7%	216	0.1%
Bumper	+10%	2.00	8.1%	278	-0.6%	0.099	2.0%	234	8.1%
BPR LWR	+10%	1.89	2.0%	274	-2.1%	0.098	0.6%	220	2.0%
Hood (Z)	+10%	1.87	1.3%	279	-0.4%	0.097	0.1%	214	-1.0%
Hood	-20%	1.84	-0.6%	277	-1.1%	0.096	-1.0%	215	-0.6%
Grille	-20%	1.81	-2.1%	260	-7.2%	0.096	-1.6%	219	1.5%
Bumper	-20%	1.60	-13.7%	264	-5.9%	0.096	-1.1%	186	-13.7%
BPR LWR	-20%	1.83	-1.1%	285	1.8%	0.099	1.9%	214	-1.1%
Hood (Z)	-20%	1.81	-2.1%	279	-0.3%	0.097	0.0%	217	0.3%
Hood	+20%	1.84	-0.7%	283	1.1%	0.099	1.7%	215	-0.7%
Grille	+20%	1.94	4.9%	303	8.1%	0.101	3.8%	215	-0.3%
Bumper	+20%	2.15	16.1%	283	1.2%	0.100	2.5%	251	16.1%
BPR LWR	+20%	1.90	2.9%	274	-2.3%	0.098	0.2%	222	2.9%

TABLE V

COMPARISONS OF INJURY MEASURES BETWEEN BASELINE MODEL AND MODELS WITH DIFFERENT STIFFNESS CURVES SCALED IN DEFLECTION FOR VEHICLE B (BPR LWR STANDS FOR BUMPER LOWER)

Component	Scaled Factor	Pelvis Deformation (mm) and Difference		Femur Bending Moment (Nm) and Difference		MCL Tensile Strain (-) and Difference		Tibia Bending Moment (Nm) and Difference	
Baseline	-	5.94	-	201	-	0.101	-	156	-
Hood	-10%	5.96	0.3%	200	-0.4%	0.101	-0.3%	156	0.1%
Grille	-10%	6.04	1.7%	201	-0.1%	0.101	0.0%	156	-0.2%
Bumper	-10%	6.04	1.6%	201	0.2%	0.101	0.4%	155	-0.6%
BPR LWR	-10%	5.93	-0.1%	200	-0.4%	0.101	0.0%	156	0.2%
Hood	+10%	6.03	1.5%	200	-0.4%	0.102	0.6%	154	-1.4%
Grille	+10%	6.02	1.4%	202	0.5%	0.101	-0.2%	157	0.4%
Bumper	+10%	5.93	-0.1%	199	-0.8%	0.101	-0.4%	155	-0.4%
BPR LWR	+10%	6.05	1.9%	200	-0.4%	0.101	0.4%	156	-0.2%
Hood	-20%	5.97	0.5%	210	4.4%	0.098	-3.1%	160	2.7%
Grille	-20%	5.93	-0.2%	201	-0.1%	0.101	0.1%	157	0.4%
Bumper	-20%	6.06	2.0%	201	0.1%	0.102	0.7%	154	-1.2%
BPR LWR	-20%	5.94	0.0%	201	-0.2%	0.101	-0.2%	156	0.1%
Hood	+20%	5.98	0.6%	201	-0.2%	0.102	1.3%	153	-1.6%
Grille	+20%	6.03	1.5%	202	0.7%	0.101	0.2%	156	0.3%
Bumper	+20%	5.90	-0.7%	200	-0.3%	0.100	-0.8%	154	-1.0%
BPR LWR	+20%	5.93	-0.1%	202	0.6%	0.101	-0.3%	156	0.0%

TABLE VI

COMPARISONS OF INJURY MEASURES BETWEEN BASELINE MODEL AND MODELS WITH DIFFERENT STIFFNESS CURVES SCALED IN FORCE FOR VEHICLE B (BPR LWR STANDS FOR BUMPER LOWER)

Component	Scaled Factor	Pelvis deformation (mm) and Difference		Femur bending moment (Nm) and Difference		MCL tensile strain (-) and Difference		Tibia bending moment (Nm) and Difference	
Baseline	-	5.94	-	201	-	0.101	-	156	-
Hood	-10%	5.60	-5.8%	206	2.7%	0.104	2.7%	156	-0.3%
Grille	-10%	5.83	-1.8%	199	-0.8%	0.101	-0.1%	153	-2.0%
Bumper	-10%	5.87	-1.2%	192	-4.5%	0.097	-3.7%	145	-6.9%
BPR LWR	-10%	5.93	-0.1%	199	-0.8%	0.101	0.2%	157	0.6%
Hood	+10%	6.39	7.5%	194	-3.3%	0.099	-2.2%	156	0.3%
Grille	+10%	6.15	3.5%	202	0.5%	0.101	0.4%	159	1.9%
Bumper	+10%	6.07	2.1%	213	6.2%	0.104	3.4%	165	5.9%
BPR LWR	+10%	5.94	0.0%	200	-0.3%	0.101	0.1%	157	0.5%
Hood	-20%	5.11	-14.0%	213	5.9%	0.106	5.3%	154	-1.0%
Grille	-20%	5.77	-2.8%	200	-0.5%	0.101	0.1%	150	-4.0%
Bumper	-20%	5.74	-3.4%	181	-9.9%	0.093	-7.8%	134	-14.1%
BPR LWR	-20%	5.94	0.0%	199	-0.8%	0.101	-0.1%	157	0.6%
Hood	+20%	6.77	13.9%	189	-5.9%	0.097	-3.7%	157	0.9%
Grille	+20%	6.16	3.6%	201	-0.1%	0.101	0.0%	162	3.6%
Bumper	+20%	6.11	2.9%	228	13.3%	0.109	7.7%	176	13.0%
BPR LWR	+20%	5.95	0.1%	201	0.0%	0.101	-0.3%	158	1.3%

TABLE VII

COMPARISONS OF INJURY MEASURES BETWEEN BASELINE MODEL AND MODELS WITH DIFFERENT STIFFNESS CURVES SCALED IN DEFLECTION FOR VEHICLE C (BPR LWR STANDS FOR BUMPER LOWER)

Component	Scaled Factor	Pelvis deformation (mm) and Difference		Femur bending moment (Nm) and Difference		MCL tensile strain (-) and Difference		Tibia bending moment (Nm) and Difference	
Baseline	-	4.00	-	201	-	0.101	-	156	-
Hood	-10%	4.10	2.6%	160	0.1%	0.076	-0.1%	197	0.3%
Grille	-10%	3.93	-1.7%	158	-1.4%	0.075	-0.8%	198	0.8%
Bumper	-10%	3.98	-0.5%	164	2.7%	0.076	0.3%	199	1.5%
BPR LWR	-10%	4.00	0.0%	160	0.1%	0.076	0.0%	196	0.0%
Hood	+10%	3.93	-1.7%	161	0.8%	0.076	0.0%	195	-0.5%
Grille	+10%	3.97	-0.7%	164	2.3%	0.077	1.4%	195	-0.6%
Bumper	+10%	4.00	0.1%	157	-1.7%	0.076	-0.2%	193	-1.3%
BPR LWR	+10%	4.01	0.3%	162	1.4%	0.076	-0.2%	197	0.3%
Hood	-20%	4.19	4.8%	160	-0.1%	0.076	0.2%	197	0.3%
Grille	-20%	3.91	-2.1%	155	-3.3%	0.075	-1.2%	200	1.8%
Bumper	-20%	3.94	-1.4%	165	3.2%	0.076	0.6%	198	1.2%
BPR LWR	-20%	3.97	-0.7%	160	-0.1%	0.076	-0.3%	195	-0.7%
Hood	+20%	3.88	-3.0%	159	-0.6%	0.076	-0.2%	196	0.0%
Grille	+20%	3.98	-0.5%	167	4.2%	0.077	1.4%	195	-0.8%
Bumper	+20%	4.04	1.1%	153	-4.1%	0.076	-0.3%	191	-2.7%
BPR LWR	+20%	4.00	0.1%	161	0.8%	0.076	0.6%	196	0.1%

TABLE VIII

COMPARISONS OF INJURY MEASURES BETWEEN BASELINE MODEL AND MODELS WITH DIFFERENT STIFFNESS CURVES SCALED IN FORCE FOR VEHICLE C (BPR LWR STANDS FOR BUMPER LOWER)

Component	Scaled Factor	Pelvis Deformation (mm) and Difference		Femur Bending Moment (Nm) and Difference		MCL Tensile Strain (-) and Difference		Tibia Bending Moment (Nm) and Difference	
Baseline	-	4.00	-	201	-	0.101	-	156	-
Hood	-10%	3.90	-2.6%	160	0.3%	0.076	0.4%	198	0.9%
Grille	-10%	3.91	-2.4%	161	0.5%	0.076	0.7%	198	1.1%
Bumper	-10%	3.96	-1.0%	147	-8.2%	0.074	-1.9%	181	-7.5%
BPR LWR	-10%	4.02	0.4%	162	1.0%	0.076	0.6%	197	0.4%
Hood	+10%	4.13	3.1%	158	-1.4%	0.076	0.3%	195	-0.6%
Grille	+10%	4.11	2.8%	160	0.0%	0.076	-0.1%	196	-0.1%
Bumper	+10%	3.99	-0.3%	172	7.3%	0.078	3.4%	209	6.5%
BPR LWR	+10%	3.99	-0.2%	161	0.4%	0.076	-0.3%	196	-0.2%
Hood	-20%	3.80	-5.0%	162	1.1%	0.076	0.2%	196	0.0%
Grille	-20%	3.76	-5.9%	162	1.2%	0.077	1.2%	197	0.4%
Bumper	-20%	3.95	-1.3%	127	-20.9%	0.071	-6.0%	163	-16.8%
BPR LWR	-20%	4.03	0.6%	164	2.6%	0.078	2.1%	197	0.6%
Hood	+20%	4.21	5.2%	160	0.3%	0.076	0.1%	197	0.4%
Grille	+20%	4.24	5.9%	159	-0.8%	0.076	-0.4%	198	0.8%
Bumper	+20%	3.89	-2.8%	183	14.7%	0.080	5.1%	228	16.4%
BPR LWR	+20%	3.95	-1.2%	162	1.1%	0.075	-0.9%	194	-1.2%

Effect of Change in Contact Area

The comparisons of the pelvis and lower limb injury measures are shown in TABLEs VIIII through XI. The differences in the peak injury measures were within the range of ±15% for all measures in H-A1-L, G-A1-U, G-A1-L and G-A3 for Vehicle A, H-A1-L, H-A2-U, G-A1-U, G-A1-L and G-A3 for Vehicle B, and H-A1-U, H-A2-U, H-A2-L, H-A3 and G-A3 for Vehicle C.

TABLE VIII

COMPARISONS OF INJURY MEASURES BETWEEN BASELINE MODEL AND MODELS WITH DIFFERENT CONTACT AREA FOR VEHICLE A

Case ID	Pelvis Deformation (mm) and Difference		Femur Bending Moment (Nm) and Difference		MCL Tensile Strain (-) and Difference		Tibia Bending Moment (Nm) and Difference	
Baseline	1.71	-	253	-	0.092	-	230	-
H-A1-U	2.46	43.9%	152	-39.9%	0.068	-25.6%	202	-12.2%
H-A1-L	1.47	-14.0%	280	10.7%	0.092	0.0%	236	2.6%
H-A2-U	1.89	10.5%	179	-29.2%	0.074	-19.6%	214	-7.0%
H-A2-L	1.31	-23.4%	221	-12.6%	0.083	-9.4%	209	-9.1%
H-A3	1.69	-1.2%	202	-20.2%	0.077	-15.5%	218	-5.2%
G-A1-U	1.6	-6.4%	249	-1.6%	0.097	5.6%	229	-0.4%
G-A1-L	1.49	-12.9%	244	-3.6%	0.101	10.8%	237	3.0%
G-A3	1.57	-8.2%	243	-4.0%	0.098	6.6%	234	1.7%
B-1-U	1.74	1.8%	310	22.5%	0.153	66.7%	218	-5.2%
B-1-L	1.67	-2.3%	239	-5.5%	0.075	-17.8%	218	-5.2%
B-A3	1.58	-7.6%	272	7.5%	0.112	22.2%	227	-1.3%

TABLE X

COMPARISONS OF INJURY MEASURES BETWEEN BASELINE MODEL AND MODELS WITH DIFFERENT CONTACT AREA FOR VEHICLE B

Case ID	Pelvis Deformation (mm) and Difference		Femur Bending Moment (Nm) and Difference		MCL Tensile Strain (-) and Difference		Tibia Bending Moment (Nm) and Difference	
Baseline	5.42	-	265	-	0.118	-	249	-
H-A1-U	5.45	0.6%	179	-32.5%	0.106	-10.4%	233	-6.4%
H-A1-L	5.78	6.6%	283	6.8%	0.106	-10.4%	252	1.2%
H-A2-U	5.62	3.7%	234	-11.7%	0.105	-11.2%	235	-5.6%
H-A2-L	5.64	4.1%	223	-15.8%	0.103	-12.8%	244	-2.0%
H-A3	5.79	6.8%	196	-26.0%	0.108	-8.8%	243	-2.4%
G-A1-U	5.7	5.2%	255	-3.8%	0.116	-2.4%	243	-2.4%
G-A1-L	5.2	-4.1%	267	0.8%	0.117	-0.8%	266	6.8%
G-A3	5.55	2.4%	256	-3.4%	0.116	-2.4%	252	1.2%
B-1-U	5.92	9.2%	367	38.5%	0.178	50.4%	227	-8.8%
B-1-L	5.21	-3.9%	178	-32.8%	0.124	4.8%	242	-2.8%
B-A3	5.73	5.7%	262	-1.1%	0.155	31.2%	213	-14.5%

TABLE XI

COMPARISONS OF INJURY MEASURES BETWEEN BASELINE MODEL AND MODELS WITH DIFFERENT CONTACT AREA FOR VEHICLE C

Case ID	Pelvis Deformation (mm) and Difference		Femur Bending Moment (Nm) and Difference		MCL Tensile Strain (-) and Difference		Tibia Bending Moment (Nm) and Difference	
Baseline	4.31	-	216	-	0.101	-	246	-
H-A1-U	3.84	-10.9%	213	-1.4%	0.100	-0.9%	248	0.8%
H-A1-L	5.39	25.1%	203	-6.0%	0.100	-0.9%	248	0.8%
H-A2-U	4.47	3.7%	211	-2.3%	0.101	0.0%	247	0.4%
H-A2-L	4.82	11.8%	207	-4.2%	0.100	-0.9%	247	0.4%
H-A3	4.56	5.8%	210	-2.8%	0.101	0.0%	248	0.8%
G-A1-U	5.24	21.6%	140	-35.2%	0.082	-18.8%	232	-5.7%
G-A1-L	3.19	-26.0%	317	46.8%	0.116	14.0%	266	8.1%
G-A3	4.38	1.6%	192	-11.1%	0.092	-9.2%	244	-0.8%
B-1-U	4.36	1.2%	392	81.5%	0.147	44.9%	220	-10.6%
B-1-L	3.72	-13.7%	151	-30.1%	0.121	19.6%	290	17.9%
B-A3	4.1	-4.9%	240	11.1%	0.149	46.7%	254	3.3%

IV. DISCUSSION

The maximum difference in the peak injury measures between the results from the baseline model and the simulations using the stiffness curves scaled in the direction of the deflection was approximately 3% and 5% when the deflection at the peak force was varied by ±10% and ±20%, respectively. In contrast, the corresponding difference for the stiffness curves scaled in the direction of the force was approximately 5% and 21% when the peak force magnitude was varied by ±10% and ±20%, respectively. This suggests that the effect of the level of the force on the injury measures is more significant than that of the deflection.

The absorbed energy up to the peak force from the stiffness curves scaled in the direction of the deflection was the same as that from the stiffness curves scaled in the direction of the force, when these parameters were varied by the same percentage. Therefore, it is also suggested that the effect of the level of the force on the injury measures is more significant than that of the absorbed energy up to the peak force.

In the cases where the contact area from the hood was varied, the difference of the peak injury measures under the range of ±30% relative to the baseline model was observed only in Vehicle C (minivan). The hood contacts the pelvis only in Vehicle C, while it contacts the pelvis and the femur in Vehicles A (sedan) and B (SUV). Therefore, a possible explanation for this could be that the injury measures do not vary significantly when the contact area varies within one body region. In the cases where the contact area from the grille was varied, the differences of the injury measures were under the range of ±15% relative to the baseline model in Vehicles A and B. This could be explained by the fact that the level of the maximum load from the grille was significantly lower than those from the hood and the bumper in the three vehicles used in this study (Fig. 15).

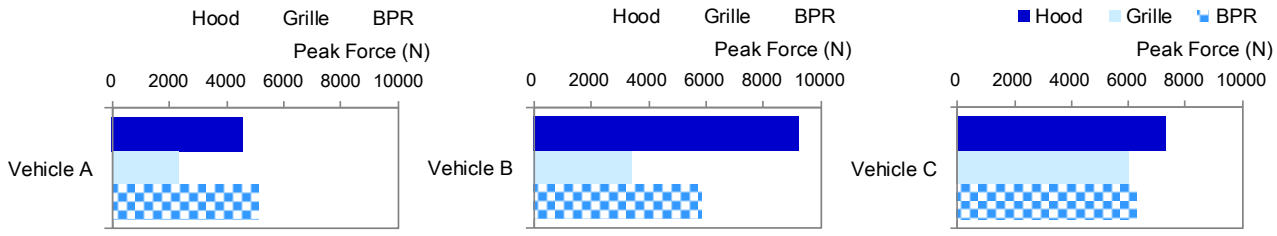

Fig. 15. Comparison of the Peak Force Magnitude from the Hood, Grille and Bumper

In order to accurately reproduce the peak injury measures, it seems to be necessary to reproduce the body regions to be loaded, regardless of the component that applies the load. Although this study only focused on a mid-sized male, it is also possible to perform a similar study using pedestrian models in different sizes. Since the difference in pedestrian anthropometry would alter the pelvis and lower limb loading mechanisms for the same vehicle, a future study would focus on the development of a guideline in the pedestrian buck development for different pedestrian sizes.

V. CONCLUSIONS

In this study, two parametric studies were conducted to clarify the effect of the difference in the stiffness characteristics and the contact area on pedestrian pelvis and lower limb injury measures. Car-pedestrian impact simulations using a human FE model and simplified vehicle models were conducted for investigating the effect of the difference in the peak force magnitude and the deflection at the peak force. In order to isolate the effect of the contact area change, the baseline Prescribed Force-Time model was developed in which prescribed force time histories were applied to the nodes on the surface of the human model located in the contact area, and the contact area was varied by maintaining the magnitude of the total applied force. As a result, the following conclusions were reached;

- The maximum injury measures were reproduced within ±5%, when the peak force magnitude was conserved and the deflection at the peak force was varied by ±20%.
- The maximum injury measures were reproduced within ±8%, when the deflection at the peak force was conserved and the peak force magnitude was varied by ±10%.

- The maximum injury measures were reproduced within ±21%, when the deflection at the peak force was conserved and the peak force magnitude was varied by ±20%.
- In order to accurately reproduce the maximum injury measures, the buck components that represent the hood, grille and bumper face should apply load to the whole area on a pedestrian body that these components are supposed to contact in an impact from the vehicle represented by the buck.

VI. REFERENCES

[1] International Traffic Safety Data and Analysis Group IRTAD Annual report 2010, [http://internationaltransportforum.org/ irtadpublic/pdf/10IrtadReport.pdf]

[2] Akiyama, A., Okamoto, M. and Rangarajan, N. Development and Application of New Pedestrian Dummy, Paper Number 463, *Proceedings of the 17th Conference on the Enhanced Safety Vehicle (ESV)*, 2001.

[3] Society of Automobile Engineers Human Biomechanics And Simulations Standards Steering Committee : Performance Specifications for a Midsize Male Pedestrian Research Dummy, Surface Vehicle Information Report J2782, 2010.

[4] Society of Automobile Engineers Human Biomechanics And Simulations Standards Steering Committee : Pedestrian Dummy Full Scale Test Results and Resource Materials, Surface Vehicle Information Report J2868, 2010.

[5] Untaroiu, C., Shin, J., Crandall, J. R., Fredriksson, R., Bostrom, O., Takahashi, Y., Akiyama, A., Okamoto, M., Kikuchi. Y. : Development and Validation of Pedestrian Sedan Bucks using Finite Element Simulations; Application in Study in the Influence of Vehicle Automatic Breaking on the Kinematics of the Pedestrian Involved in Vehicle Collisions, *Proceedings of 21st ESV Conference*, Paper Number 09-0485, 2009.

[6] Suzuki, S., Takahashi, Y., Okamoto, M., Fredriksson, R., Oda, S. , Validation of a Pedestrian Sedan Buck Using a Human Finite Element Model, *Proceedings of 22nd ESV Conference*, Paper Number 11-0277, 2011.

[7] Takahashi, Y., Suzuki, S., Oda, S., Frederiksson, R., Pipkorn, B., Effect of Stiffness Characteristics of Vehicle Front-end Structures on Pedestrian Pelvis and Lower Limb Injury Measures, *Proceedings of IRCOBI Conference*, 2011.

[8] Takahashi, Y., Suzuki, S., Okamoto, M., Oda, S., Investigation of the Effect of Stiffness Characteristics of Vehicles on Pedestrian Pelvis and Lower Limb Injury Measures, *Transactions of Society of Automotive Engineers of Japan (JSAE)*, Vol. 43 No.2, 20124216, 2011. (in Japanese)

[9] Takahashi, Y., Suzuki, S., Ikeda, M., Gunji, Y. , Investigation on Pedestrian Pelvis Loading Mechanisms Using Finite Element Simulations, *Proceedings of IRCOBI Conference*, 2010.

[10] Ikeda, M., Suzuki, S., Gunji, Y., Takahashi, Y., Motozawa, Y., Hitosugi, M., Development of An Advanced Finite Element Model for A Pedestrian Pelvis, *Proceedings of 22nd ESV Conference*, Paper Number 11-0009, 2011